Data-driven estimation of spatial electrical property of multi-compartment models with neuronal morphology by replica exchange Monte Carlo method

Nakano, Hirozo

Majumdar, Amitava

Omori, Toshiaki

(Citation)
Nonlinear Theory and Its Applications, IEICE,15(2):389-403

(Issue Date)
2024-04-01

(Resource Type)
journal article

(Version)
Version of Record

NOLTA, IEICE

Paper

Data-driven estimation of spatial electrical property of multi-compartment models with neuronal morphology by replica exchange Monte Carlo method

Hirozo Nakano[1], *Amitava Majumdar*[2], and *Toshiaki Omori*[1,3,4a)]

[1] *Graduate School of Engineering, Kobe University 1–1 Rokkodai-cho, Nada-ku, Kobe, Hyogo 657-8501, Japan*

[2] *San Diego Supercomputer Center, University of California San Diego 9500 Gilman Drive, La Jolla, California, 92093, United States of America*

[3] *Center for Mathematical and Data Sciences, Kobe University 1–1 Rokkodai-cho, Nada-ku, Kobe, Hyogo 657-8501, Japan*

[4] *Center of Optical Scattering Image Science, Kobe University 1–1 Rokkodai-cho, Nada-ku, Kobe, Hyogo 657-8501, Japan*

[a)] *omori@eedept.kobe-u.ac.jp*

Received October 17, 2023; Revised December 15, 2023; Published April 1, 2024

Abstract: One of the neuron models that simulate the electrical activity of neurons, the multi-compartment model, has spatial electrical properties that control nonlinear spatiotemporal dynamics and can reproduce nonlinear electrical responses with high accuracy. However, it is difficult to determine the model parameters in multi-compartment models from membrane potentials, since unknown high dimensional parameters for spatial electrical property should be estimated using incomplete observation data. In this paper, we propose a data-driven method to estimate the spatial electrical properties in the multi-compartment model from membrane potentials observed incompletely. The proposed method employs the replica exchange method using prior information considering morphological smoothness to solve problems of the local optima in the solution space and incompleteness of observation data. We further verify the effectiveness of the proposed method by using simulation data obtained from realistic neuron models.

Key Words: inverse-problem, multi-compartment model, nonlinear dynamics, statistical machine learning, neural dynamics, neuroscience

1. Introduction

Extracting nonlinear spatiotemporal dynamics in neurons is one of the most important issues for understanding information processing in the brain. From recent researches, it is known to that spatial structure of dendrites plays an important role in information processing in single neurons and local neural circuits [1, 2]. For example, the apical dendrites in the hippocampal CA1 pyramidal neurons receive synaptic inputs from adjacent area called the hippocampal CA3, whereas its distal dendrites receive synaptic inputs from more distinct area called the entorhinal cortex [3]. Moreover, in addition to spatial structure of dendrites, it is known that spatial characteristics of electrical properties in dendrites affect nonlinear spatiotemporal dynamics in neurons. For example, multiple types of voltage-gated ion channels in Purkinje cells make complex spikes in neurons [4]. Recent research suggests that neurons perform complex computation such as detecting synchronized inputs [5], selecting inputs [6] and calculating expected values [7] by applying nonlinear spatiotemporal transformations to synaptic inputs in dendrites. Therefore, it is important to estimate spatial electrical properties of neurons for understanding information processing in the brain.

Due to developments in imaging technology, nonlinear spatiotemporal dynamics in neurons has been recorded as imaging data extensively [8–10]. By using fluorescence imaging, membrane potentials within dendrites can be measured from multiple points at the same time. However, membrane potentials are partially observable because of limitations of spatial resolution for neural imaging. Moreover, membrane potentials are noisy because of observation noise.

In order to extract spatiotemporal neuronal dynamics, it is necessary to establish data-driven framework for estimating spatial electrical properties from membrane potentials. Prior works have proposed framework for estimating parameters of neuron models that ignore spatial structure of neurons [11–13], such as the Hodgkin-Huxley model [14] and Izhikevich model [15]. In contrast, estimating spatial electrical properties that reproduce nonlinear spatiotemporal electrical activity in neurons has been difficult due to 1) morphological characteristics, where dendrites of neurons have complicated shapes; 2) complex energy structure, where incorrect properties are estimated because of being stuck in local optima; 3) incomplete observation data, where membrane potentials are partially observable and noisy.

In this paper, we propose a data-driven method based on the replica exchange method [16, 17] to estimate spatial electrical properties in the multi-compartment model from membrane potentials observed incompletely. The multi-compartment model [18], one of the neuron models, is known to have spatial electrical properties and reproduce nonlinear dynamics in neurons with high accuracy. We also formulate a data-driven framework based on replica exchange method with prior distribution considering morphological smoothness for estimating the spatial electrical properties in the multi-compartment model. Furthermore, we evaluate the proposed method through numerical experiments using simulated data generated from realistic neuron models.

2. Method

In this section, we propose the data-driven framework for estimating spatial electrical properties of a neuron model from incomplete observation data. First, we explain the multi-compartment model that represents the nonlinear spatiotemporal dynamics of electrical activity in neurons. Next, we formulate posterior probability for estimating model parameters, and propose the data-driven framework based on replica exchange Monte Carlo method with prior information considering morphological for estimating model parameters. Finally, we show the algorithm for estimating spatial electrical properties in the situation that the membrane potentials are incompletely observed.

2.1 Multi-compartment model

The multi-compartment model is one of the neuron models that represents the nonlinear spatiotemporal dynamics of electrical activity in neurons. Neuron models described by using the multi-compartment model are divided into small segments called compartments as shown in Fig. 1. In contrast to other neuron models, the multi-compartment model has nonlinear response property at each position called compartment and forms spatial electrical properties, thus we can consider the

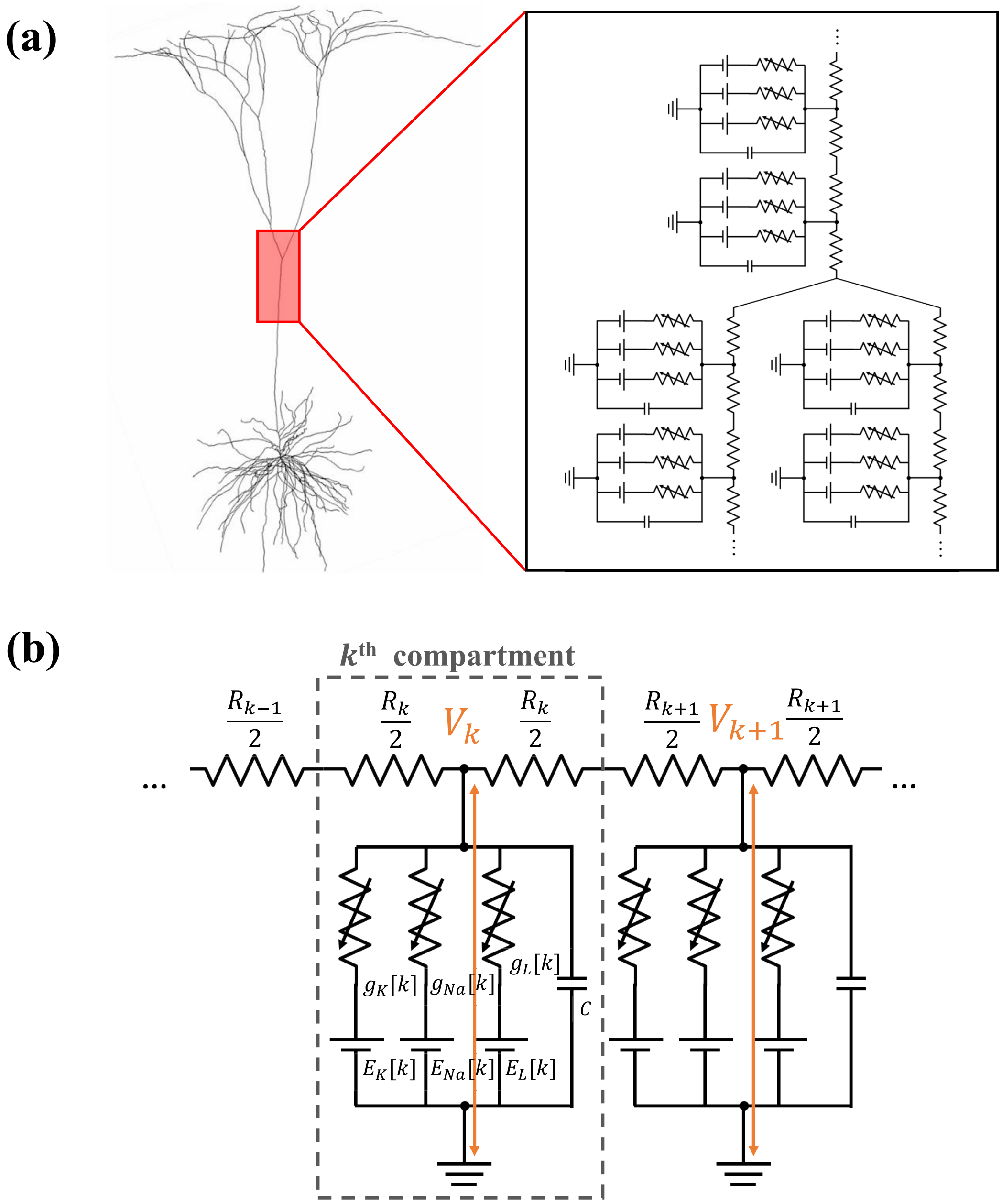

Fig. 1. Neuron described by using the multi-compartment model. (a) The multi-compartment model divides neurons into small segments called compartments. (b) Membrane potential at each compartment is governed by membrane currents and intracellular currents between neighboring compartments.

shape of neurons. Nonlinear response in each compartment propagates to other compartments along dendrites as electrical response. Therefore, the multi-compartment neuron model can reproduce the nonlinear spatiotemporal electrical response of neurons with high accuracy.

The membrane potential of the kth compartment V_k is represented by the following differential equation:

$$
\begin{aligned}
C\frac{dV_k}{dt} =& -g_L^{(k)}(V_k - E_L^{(k)}) - g_{Na}^{(k)} m_k^3 h_k (V_k - E_{Na}^{(k)}) - g_K^{(k)} n_k^4 (V_k - E_K^{(k)}) \\
&- \sum_{k' \in N_k} \frac{1}{R^{(k,k')}}(V_k - V_{k'}) + I_k(t)
\end{aligned}
\tag{1}
$$

where C is membrane capacity, $g_L^{(k)}$, $g_{Na}^{(k)}$ and $g_K^{(k)}$ are leak, Na^+ and K^+ maximal electrical conductances and $E_L^{(k)}$, $E_{Na}^{(k)}$ and $E_K^{(k)}$ are leak, Na^+ and K^+ reversal potentials. The first, second, and third terms represent leakage current and membrane currents with sodium-ion and potassium-ion concentration. Here, m_k, h_k, n_k in Eq. (1) are channel variables given by the following differential equations:

$$\frac{dm_k}{dt} = \alpha_m(V_k)(1-m_k) - \beta_m(V_k)m_k \tag{2}$$

$$\frac{dh_k}{dt} = \alpha_h(V_k)(1-h_k) - \beta_h(V_k)h_k \tag{3}$$

$$\frac{dn_k}{dt} = \alpha_n(V_k)(1-n_k) - \beta_n(V_k)n_k \tag{4}$$

where $\alpha_x(V_k)$ and $\beta_x(V_k)$ ($x \in \{m,h,n\}$) are nonlinear functions. The fourth term of Eq. (1) represents the intracellular currents due to the influence of adjacent compartments. N_k denotes the set of compartments adjacent to the kth compartment and $R^{(k,k')}$ denotes the internal resistance between kth and k'th compartments. $I_k(t)$ is the external input current. There are seven parameters $\boldsymbol{\theta} = \{g_L^{(k)}, E_L^{(k)}, g_{Na}^{(k)}, E_{Na}^{(k)}, g_K^{(k)}, E_K^{(k)}, R^{(k,k')}\}$ in the multi-compartment model, and the multi-compartment models with different values of parameters $\boldsymbol{\theta}$ can represent various nonlinear spatiotemporal electrical responses of neurons by adjusting these parameters. Therefore, by using the multi-compartment model, we can consider complicated shape of neurons and nonlinear spatiotemporal dynamics in neurons.

In this study, membrane potentials are assumed to be partially observable and noisy. Here, we assume that observation data $\boldsymbol{D}_{1:L}$ is given by the following equation through noisy observation as follows:

$$\boldsymbol{D}_{1:L} = \{V_k + \varepsilon_k; k \in \boldsymbol{\mathcal{O}}\} \tag{5}$$

where ε_k is observation noise and $\boldsymbol{\mathcal{O}}$ is a subset of compartments. We assume that membrane potentials at limited compartments can be observed at discretized time steps ($t = 1, 2, \cdots, L$).

2.2 Data-driven framework for estimating spatial electrical properties by using replica exchange method with the prior distribution considering morphological smoothness

We propose data-driven framework for estimating the model parameters $\boldsymbol{\theta} = \{g_L^{(k)}, E_L^{(k)}, g_{Na}^{(k)}, E_{Na}^{(k)}, g_K^{(k)}, E_K^{(k)}, R^{(k,k')}\}$ in the multi-compartment model from spatiotemporal observed electrical activity by replica exchange method. Figure 2 shows the diagram of estimation framework. As shown in Fig. 2, the proposed method estimates spatial electrical properties $\boldsymbol{\theta}$ from membrane potentials observed incompletely $\boldsymbol{D}_{1:L}$ by generating samples following posterior distribution $p(\boldsymbol{\theta}|\boldsymbol{D}_{1:L})$.

The replica exchange method is one of the Markov chain Monte Carlo methods, and can obtain samples from the joint posterior distribution:

$$p(\boldsymbol{\theta}_{T_1}, ..., \boldsymbol{\theta}_{T_M}|\boldsymbol{D}_{1:L}) = \prod_{m=1}^{M} p(\boldsymbol{\theta}_{T_m}|\boldsymbol{D}_{1:L}, T_m) \tag{6}$$

where $T_1, ..., T_M$ are temperatures that characterize the posterior distribution $p(\boldsymbol{\theta}_{T_m}|\boldsymbol{D}_{1:L}, T_m)$ and $\boldsymbol{D}_{1:L}$ denotes observation data of spatiotemporal membrane potentials. By using replica exchange method, we can search globally in the parameter space in the high temperature, whereas we can search locally for the parameter space in low temperature. In our study, we estimate the posterior probability $p(\boldsymbol{\theta}_{T_1}|\boldsymbol{D}_{1:L}, T_1)$ at lowest temperature $T_1 = 1$ by collecting samples obtained by the replica exchange method.

In this study, the likelihood function $P(\boldsymbol{D}_{1:L}|\boldsymbol{\theta}_{T_m}, T_m)$ is determined by using the discrepancy between observation data $\boldsymbol{D}_{1:L}$ and simulation data $\hat{\boldsymbol{V}}(\boldsymbol{\theta}_{T_m})$. The likelihood function at temperature T_m is expressed by the following equation:

$$\begin{aligned} P(\boldsymbol{D}_{1:L}|\boldsymbol{\theta}_{T_m}, T_m) &= \frac{1}{(\sqrt{2\pi})^n \sigma^n} \exp\left(-\alpha_1 \frac{(\boldsymbol{D}_{1:L} - \hat{\boldsymbol{V}}(\boldsymbol{\theta}_{T_m}))^T(\boldsymbol{D}_{1:L} - \hat{\boldsymbol{V}}(\boldsymbol{\theta}_{T_m}))}{LT_m}\right) \\ &\propto \exp(-\alpha_1 E(\boldsymbol{\theta}_{T_m})) \end{aligned} \tag{7}$$

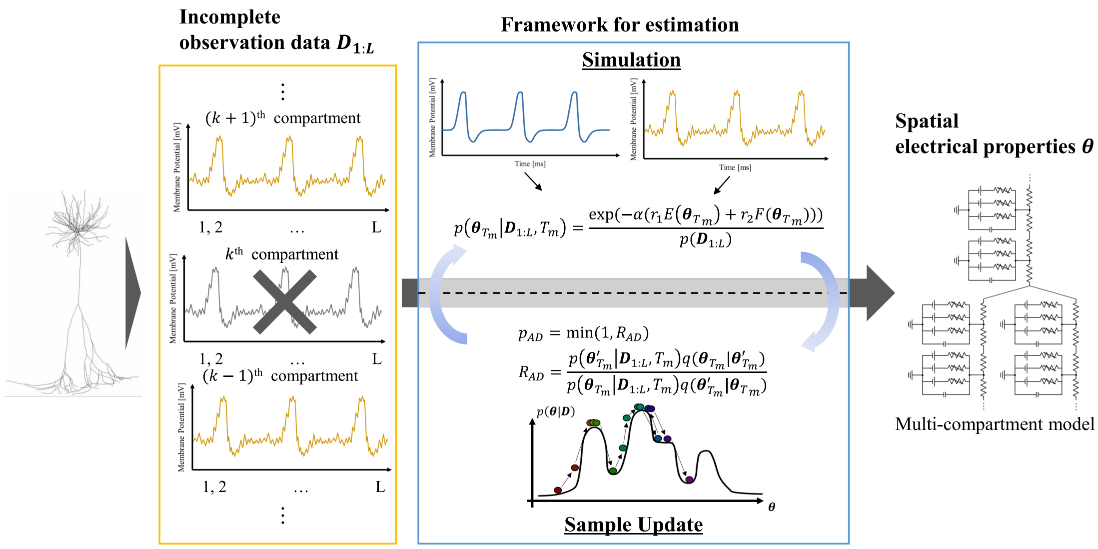

Fig. 2. Framework of the proposed method. We propose data-driven framework for estimating spatial electrical properties $\boldsymbol{\theta}$ in the multi-compartment model from the membrane potentials observed incompletely $\boldsymbol{D}_{1:L}$.

where $\alpha_1(>0)$ is the hyperparameter that controls how large we evaluate discrepancy. Simulation data $\hat{\boldsymbol{V}}(\boldsymbol{\theta}_{T_m})$ is obtained by calculating the discretized differential equation Eqs. (1)–(4). By using multi-compartment model, we can obtain more accurate spatiotemporal electrical activity in neurons. In this study, we use NEURON simulator in order to obtain membrane potentials of multi-compartment models for realistic neurons as simulation data [19].

We consider the prior distribution $p(\boldsymbol{\theta})$ by assuming the smoothness of the parameters $\boldsymbol{\theta}^{(k)}$ and $\boldsymbol{\theta}^{(k')}$ of neighboring compartments. The prior distribution $p(\boldsymbol{\theta})$ is expressed by the following equation:

$$\begin{aligned} p(\boldsymbol{\theta}) &\propto \exp\left(-\alpha_2 \sum_{k=1}^{K}\sum_{k'=1}^{K} G(\boldsymbol{\theta}^{(k)}, \boldsymbol{\theta}^{(k')})\right) \\ &= \exp(-\alpha_2 F(\boldsymbol{\theta})) \end{aligned} \tag{8}$$

$$G(\boldsymbol{\theta}^{(k)}, \boldsymbol{\theta}^{(k')}) = \begin{cases} |\boldsymbol{\theta}^{(k)} - \boldsymbol{\theta}^{(k')}| & \text{if} \quad k' \in N_k \\ 0 & \text{otherwise} \end{cases} \tag{9}$$

where $\alpha_2(>0)$ is the hyperparameter that controls how strong we impose constrains of prior information. Equation (8) corresponds to prior information for the spatial smoothness of parameters between neighboring compartments, allowing accurate model parameter estimation when complete observation data are not observable. In other words, prior considering morphological smoothness can compensate lack of observed information.

From Bayes' theorem, the posterior probability $p(\boldsymbol{\theta}_{T_m}|\boldsymbol{D}_{1:L}, T_m)$ of the parameters expressed by the following equation:

$$p(\boldsymbol{\theta}_{T_m}|\boldsymbol{D}_{1:L}, T_m) = \frac{\exp\left(-\left(\alpha_1 E(\boldsymbol{\theta}_{T_m}) + \alpha_2 F(\boldsymbol{\theta}_{T_m})\right)\right)}{p(\boldsymbol{D}_{1:L})} \tag{10}$$

where $p(\boldsymbol{D}_{1:L})$ is the marginal distribution.

We derive two types of Markov chain whose samples follow posterior distribution $p(\boldsymbol{\theta}|\boldsymbol{D}_{1:L}, T_m)$. Here we consider a set of parameters $\Theta = \{\boldsymbol{\theta}_{T_1}, \cdots, \boldsymbol{\theta}_{T_i}, \cdots, \boldsymbol{\theta}_{T_j}, \cdots, \boldsymbol{\theta}_{T_M}\}$ at different temperatures $\mathcal{T} = \{T_1, \cdots, T_i, \cdots, T_j, \cdots, T_M\}$, and changes of samples within the same temperature and exchange of samples between different temperatures from the detailed balance [20, 21]:

$$p(\Theta|\boldsymbol{D}_{1:L}, \mathcal{T})w(\Theta \to \Theta'|\boldsymbol{D}_{1:L}, \mathcal{T}) = p(\Theta'|\boldsymbol{D}_{1:L}, \mathcal{T})w(\Theta' \to \Theta|\boldsymbol{D}_{1:L}, \mathcal{T}) \tag{11}$$

where $p(\Theta|\boldsymbol{D}_{1:L}, \mathcal{T})$ is the joint posterior probability and $w(\Theta \to \Theta'|\boldsymbol{D}_{1:L}, \mathcal{T})$ is the transition probability from Θ to Θ' conditioned on observation data $\boldsymbol{D}_{1:L}$ and the set of temperatures $\mathcal{T}$. Hereafter, we omit $\boldsymbol{D}_{1:L}$ and $\mathcal{T}$ in $w(\cdot)$ for simplicity. In order to sample from $p(\Theta|\boldsymbol{D}_{1:L},\mathcal{T})$, transition probability $w(\cdot)$ must satisfy Eq. (11).

First, we consider sample changes within the same temperature. From Eq. (11), the detailed balance of sample changes within the same temperature T_i is expressed by the following equation:

$$p(\boldsymbol{\theta}_{T_i}|\boldsymbol{D}_{1:L},T_i)w(\boldsymbol{\theta}_{T_i}\to\boldsymbol{\theta}'_{T_i}) = p(\boldsymbol{\theta}'_{T_i}|\boldsymbol{D}_{1:L},T_i)w(\boldsymbol{\theta}'_{T_i}\to\boldsymbol{\theta}_{T_i}) \tag{12}$$

where $w(\boldsymbol{\theta}_{T_i}\to\boldsymbol{\theta}'_{T_i})$ is the transition probability of parameter at temperature T_i. Here, we consider sampling of parameters $\boldsymbol{\theta}'_{T_i}$ using the probability $\rho(\boldsymbol{\theta}'_{T_i}|\boldsymbol{\theta}_{T_i})$ that corresponds to the probability that parameters $\boldsymbol{\theta}'_{T_i}$ are picked up. The transition probability $w(\boldsymbol{\theta}_{T_i}\to\boldsymbol{\theta}'_{T_i})$ is expressed by the following equation:

$$w(\boldsymbol{\theta}_{T_i}\to\boldsymbol{\theta}'_{T_i}) = \begin{cases} 1\cdot\rho(\boldsymbol{\theta}'_{T_i}|\boldsymbol{\theta}_{T_i}) & \text{if } p(\boldsymbol{\theta}_{T_i}|\boldsymbol{D}_{1:L},T_i) < p(\boldsymbol{\theta}'_{T_i}|\boldsymbol{D}_{1:L},T_i) \\ \frac{p(\boldsymbol{\theta}'_{T_i}|\boldsymbol{D}_{1:L},T_i)\rho(\boldsymbol{\theta}_{T_i}|\boldsymbol{\theta}'_{T_i})}{p(\boldsymbol{\theta}_{T_i}|\boldsymbol{D}_{1:L},T_i)\rho(\boldsymbol{\theta}'_{T_i}|\boldsymbol{\theta}_{T_i})}\cdot\rho(\boldsymbol{\theta}'_{T_i}|\boldsymbol{\theta}_{T_i}) & \text{otherwise} \end{cases} \tag{13}$$

Here, we assume that we definitely accept sample changes $\boldsymbol{\theta}_{T_i}\to\boldsymbol{\theta}'_{T_i}$ if $\boldsymbol{\theta}'_{T_i}$ is better samples than $\boldsymbol{\theta}_{T_i}$. Equation (13) below is derived to satisfy Eq. (12) when parameters $\boldsymbol{\theta}'_{T_i}$ are picked up with probability $\rho(\boldsymbol{\theta}'_{T_i}|\boldsymbol{\theta}_{T_i})$. Here, the probability that sample changes of parameters $\boldsymbol{\theta}'_{T_i}$ are accepted p_{AC} is expressed by the following equation:

$$p_{AC} = \min(1, R_{AC}) \tag{14}$$

$$R_{AC} = \frac{p(\boldsymbol{\theta}'_{T_i}|\boldsymbol{D}_{1:L},T_i)\rho(\boldsymbol{\theta}_{T_i}|\boldsymbol{\theta}'_{T_i})}{p(\boldsymbol{\theta}_{T_i}|\boldsymbol{D}_{1:L},T_i)\rho(\boldsymbol{\theta}'_{T_i}|\boldsymbol{\theta}_{T_i})} \tag{15}$$

Namely, we generate candidate samples from the probability $\rho(\boldsymbol{\theta}'_{T_i}|\boldsymbol{\theta}_{T_i})$ and adopt candidate samples with probability p_{AC}. As expressed in Eqs. (14) and (15), we definitely adopt better candidate samples, whereas we adopt worse candidate samples with probability determined by using the ratio of the posterior probabilities at temperature T_i.

Next, we consider exchange of samples between different temperatures. From Eq. (11), the detailed balance of sample exchange between different temperatures T_i and T_j is expressed by the following equation:

$$\begin{aligned} &p(\{\boldsymbol{\theta}_{T_i},\boldsymbol{\theta}_{T_j}\}|\boldsymbol{D}_{1:L},\{T_i,T_j\})w(\{\boldsymbol{\theta}_{T_i},\boldsymbol{\theta}_{T_j}\}\to\{\boldsymbol{\theta}_{T_j},\boldsymbol{\theta}_{T_i}\}) \\ &= p(\{\boldsymbol{\theta}_{T_j},\boldsymbol{\theta}_{T_i}\}|\boldsymbol{D}_{1:L},\{T_i,T_j\})w(\{\boldsymbol{\theta}_{T_j},\boldsymbol{\theta}_{T_i}\}\to\{\boldsymbol{\theta}_{T_i},\boldsymbol{\theta}_{T_j}\}) \end{aligned} \tag{16}$$

where $w(\{\boldsymbol{\theta}_{T_i},\boldsymbol{\theta}_{T_j}\}\to\{\boldsymbol{\theta}_{T_j},\boldsymbol{\theta}_{T_i}\})$ is the transition probability from $\boldsymbol{\theta}_{T_i}$ to $\boldsymbol{\theta}_{T_j}$ at temperature T_i and from $\boldsymbol{\theta}_{T_j}$ to $\boldsymbol{\theta}_{T_i}$ at temperature T_j. Here, we consider exchange of parameters $\boldsymbol{\theta}_{T_i}$ and $\boldsymbol{\theta}_{T_j}$ using the probability $\rho(\{\boldsymbol{\theta}_{T_j},\boldsymbol{\theta}_{T_i}\}|\{\boldsymbol{\theta}_{T_i},\boldsymbol{\theta}_{T_j}\})$ conditioned on parameters $\boldsymbol{\theta}_{T_i}$ and $\boldsymbol{\theta}_{T_j}$. We assume that $\rho(\{\boldsymbol{\theta}_{T_j},\boldsymbol{\theta}_{T_i}\}|\{\boldsymbol{\theta}_{T_i},\boldsymbol{\theta}_{T_j}\})$ is the probability that parameters $\boldsymbol{\theta}_{T_i}$ and $\boldsymbol{\theta}_{T_j}$ are picked up as a candidate for exchange. The transition probability $w(\{\boldsymbol{\theta}_{T_i},\boldsymbol{\theta}_{T_j}\}\to\{\boldsymbol{\theta}_{T_j},\boldsymbol{\theta}_{T_i}\})$ is expressed by the following equation:

$$\begin{aligned} &w(\{\boldsymbol{\theta}_{T_i},\boldsymbol{\theta}_{T_j}\}\to\{\boldsymbol{\theta}_{T_j},\boldsymbol{\theta}_{T_i}\}) \\ &= \begin{cases} 1\cdot\rho(\{\boldsymbol{\theta}_{T_j},\boldsymbol{\theta}_{T_i}\}|\{\boldsymbol{\theta}_{T_i},\boldsymbol{\theta}_{T_j}\}) & \text{if } p(\{\boldsymbol{\theta}_{T_i}\boldsymbol{\theta}_{T_j}\}|\boldsymbol{D}_{1:L},\{T_i,T_j\}) < p(\{\boldsymbol{\theta}_{T_j},\boldsymbol{\theta}_{T_i}\}|\boldsymbol{D}_{1:L},\{T_i,T_j\}) \\ \frac{p(\{\boldsymbol{\theta}_{T_j},\boldsymbol{\theta}_{T_i}\}|\boldsymbol{D}_{1:L},\{T_i,T_j\})\rho(\{\boldsymbol{\theta}_{T_i},\boldsymbol{\theta}_{T_j}\}|\{\boldsymbol{\theta}_{T_j},\boldsymbol{\theta}_{T_i}\})}{p(\{\boldsymbol{\theta}_{T_i},\boldsymbol{\theta}_{T_j}\}|\boldsymbol{D}_{1:L},\{T_i,T_j\})\rho(\{\boldsymbol{\theta}_{T_j},\boldsymbol{\theta}_{T_i}\}|\{\boldsymbol{\theta}_{T_i},\boldsymbol{\theta}_{T_j}\})}\cdot\rho(\{\boldsymbol{\theta}_{T_j},\boldsymbol{\theta}_{T_i}\}|\{\boldsymbol{\theta}_{T_i},\boldsymbol{\theta}_{T_j}\}) & \text{otherwise} \end{cases} \end{aligned} \tag{17}$$

Here, we assume that we definitely accept exchange of samples $\{\boldsymbol{\theta}_{T_i},\boldsymbol{\theta}_{T_j}\}\to\{\boldsymbol{\theta}_{T_j},\boldsymbol{\theta}_{T_i}\}$ if $\{\boldsymbol{\theta}_{T_j},\boldsymbol{\theta}_{T_i}\}$ is better samples than $\{\boldsymbol{\theta}_{T_i},\boldsymbol{\theta}_{T_j}\}$. Equation (17) below is derived to satisfy Eq. (16) when parameters $\boldsymbol{\theta}_{T_i}$ and $\boldsymbol{\theta}_{T_j}$ are picked up as a candidate for exchange with probability $\rho(\{\boldsymbol{\theta}_{T_j},\boldsymbol{\theta}_{T_i}\}|\{\boldsymbol{\theta}_{T_i},\boldsymbol{\theta}_{T_j}\})$. The probability that the sample exchange of parameters $\boldsymbol{\theta}_{T_i}$ and $\boldsymbol{\theta}_{T_j}$ is accepted p_{EX} is expressed by the following equation:

$$p_{EX} = \min(1, R_{EX}) \tag{18}$$

$$\begin{aligned} R_{EX} &= \frac{p(\{\boldsymbol{\theta}_{T_j}, \boldsymbol{\theta}_{T_i}\}|\boldsymbol{D}_{1:L}, \{T_i, T_j\})\rho(\{\boldsymbol{\theta}_{T_i}, \boldsymbol{\theta}_{T_j}\}|\{\boldsymbol{\theta}_{T_j}, \boldsymbol{\theta}_{T_i}\})}{p(\{\boldsymbol{\theta}_{T_i}, \boldsymbol{\theta}_{T_j}\}|\boldsymbol{D}_{1:L}, \{T_i, T_j\})\rho(\{\boldsymbol{\theta}_{T_j}, \boldsymbol{\theta}_{T_i}\}|\{\boldsymbol{\theta}_{T_i}, \boldsymbol{\theta}_{T_j}\})} \\ &= \frac{p(\boldsymbol{\theta}_{T_j}|\boldsymbol{D}_{1:L}, T_i)p(\boldsymbol{\theta}_{T_i}|\boldsymbol{D}_{1:L}, T_j)\rho(\{\boldsymbol{\theta}_{T_i}, \boldsymbol{\theta}_{T_j}\}|\{\boldsymbol{\theta}_{T_j}, \boldsymbol{\theta}_{T_i}\})}{p(\boldsymbol{\theta}_{T_i}|\boldsymbol{D}_{1:L}, T_i)p(\boldsymbol{\theta}_{T_j}|\boldsymbol{D}_{1:L}, T_j)\rho(\{\boldsymbol{\theta}_{T_j}, \boldsymbol{\theta}_{T_i}\}|\{\boldsymbol{\theta}_{T_i}, \boldsymbol{\theta}_{T_j}\})} \end{aligned} \tag{19}$$

Here, in the proposed method $\rho(\{\boldsymbol{\theta}_{T_j}, \boldsymbol{\theta}_{T_i}\}|\{\boldsymbol{\theta}_{T_i}, \boldsymbol{\theta}_{T_j}\})$ is set to be unity. As expressed by Eq. (18), we exchange samples $\boldsymbol{\theta}_{T_i}$ and $\boldsymbol{\theta}_{T_j}$ within different temperatures T_i and T_j with probability p_{EX}. We definitely exchange samples when a sample at high temperature is better than a sample at low temperature. On the other hand, we accept exchange of samples that samples at low temperature get worse with probability determined by using the ratio of the joint posterior probabilities of two temperatures.

By iterating two types of state changes, we samples from posterior distribution $p(\boldsymbol{\theta}|\boldsymbol{D}_{1:L}, T_m)$ at each temperature. Here, we discard initial samples in the burn-in period, the interval that samples depend on initial distribution [22].

Algorithm 1 summarizes the algorithm of the replica exchange method with prior considering morphological smoothness for estimating parameters of multi-compartment model. The proposed method employs two techniques: replica exchange and prior considering morphological smoothness.

First technique, replica exchange, contributes to efficient search in solution space. Effectiveness of replica exchange can be explained from two points: escaping from local minimum and efficient search of the parameter space. Firstly, as shown in Fig. 2, replicas at higher temperatures are more likely to accept samples with worse results than replicas at lower temperatures, and thus can be expected to escape from local minimum. The replica exchange method allows efficient search while avoiding being stuck in a local optima by exchanging samples within different temperatures [17]. Secondly, replicas at higher temperatures search the parameter space globally, and provide better candidate parameter space for replicas at lower temperatures by exchanging samples. Therefore, we can search the parameter space locally in low temperature in contrast to global search of the parameter space in high temperature. The replica exchange method allows efficient search while exchanging candidate parameter space between high and low temperatures.

Second technique, prior considering morphological smoothness constrains parameters to be spatially smooth. By using prior considering morphological smoothness, we can compensate incompleteness of observation data, and accurate model parameter can be estimated even if complete observation data are not observable.

In summary, the proposed method employs two techniques, replica exchange and prior considering morphological smoothness contribute to estimate accurate spatial electrical properties in the multi-compartment model efficiently in situation where membrane potentials are observed incompletely. In addition, the parallel computation of sample changes at different temperatures can contribute to the reduction of computation time.

3. Results

In this section, we verify the effectiveness of the proposed method: replica exchange method with the prior considering morphological smoothness. We estimate spatial electrical properties for the single branch neuron model and realistic neuron model by using simulation data. We assume that only noisy membrane potentials are partially observable.

3.1 Neuron model with single branch point

First, we estimate spatial electrical properties for conductance of leak channels $\boldsymbol{\theta} = \{g_L^{(1)}, ..., g_L^{(30)}\}$ by using the proposed method on simulation data obtained from the neuron model with the single branch point. We use the neuron described by using multi-compartment model with 30 compartments. We assume that the correct neuron model has different spatial electrical properties for different positions: following by distance from the soma at the branch as shown in Fig. 4. In one branch, the conductance of the leak channel increases as the distance from the branch point increases. In other branch, the

Algorithm 1 Data-driven framework for estimating spatial electrical properties in multi-compartment models by using replica exchange method with prior considering morphological smoothness

generate initial samples of parameters $\boldsymbol{\theta}_{T_j}[0] = [\theta_{T_j}^{(1)}, ..., \theta_{T_j}^{(K)}]$ at each temperature $T_1, ..., T_M$
for $i = 1, ..., N$ (N is the iterations of sample update) **do**
  for $j = 1, ..., M$ (M is the number of temperatures) **do**
    for $k = 1, ..., K$ (K is the number of parameters) **do**
      generate candidate samples of parameters $\boldsymbol{\theta}_{T_j}^{(k)}[*]$ with Eq. (20)
      obtain simulation data of spatiotemporal electrical activity $\hat{\boldsymbol{V}}(\boldsymbol{\theta}_{T_m})$ by using multi-compartment model
      calculate acceptance probability p_{AC} with Eq. (14)
      draw a uniform random number α_{AC} with range $[0, 1)$
      if $\alpha_{AC} \leq p_{AC}$ **then**
        $\boldsymbol{\theta}_{T_j}^{(k)}[i+1] \leftarrow \boldsymbol{\theta}_{T_j}^{(k)}[*]$
      else
        $\boldsymbol{\theta}_{T_j}^{(k)}[i+1] \leftarrow \boldsymbol{\theta}_{T_j}^{(k)}[i]$
      end if
    end for
  end for
  if samples are updated N_{EX} times **then**
    pick up replica numbers for exchange
    calculate exchange probability p_{EX} with Eq. (18)
    draw a uniform random number α_{EX} with range $[0, 1)$
    if $\alpha_{EX} \leq p_{EX}$ **then**
      $\boldsymbol{\theta}_{T_m}[i] \leftarrow \boldsymbol{\theta}_{T_{m'}}[i]$
      $\boldsymbol{\theta}_{T_{m'}}[i] \leftarrow \boldsymbol{\theta}_{T_m}[i]$
    end if
  end if
end for
discard burn-in period samples $\boldsymbol{\theta}_{T_0}[1], ..., \boldsymbol{\theta}_{T_0}[t_0]$

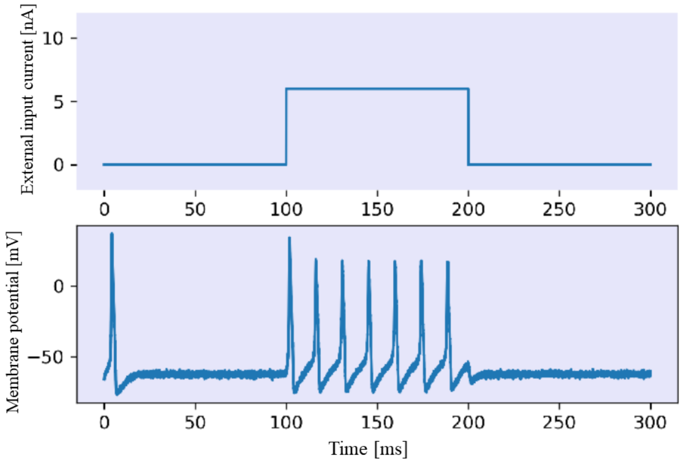

Fig. 3. External input current and observed membrane potentials. In the graph, external input current into the 10th compartment $I_{10}(t)$ (top) and observed membrane potentials in 1st compartment $\boldsymbol{D}_{1:L}[1]$ (bottom) are shown.

conductance decreases as the distance from the branch point increases. Figure 3 shows the example of observation data. We obtain membrane potentials by simulation that the four compartments are stimulated separately by $I_k(t) = 6.0\,[\text{nA}]$ for $100\,[\text{ms}]$ within $300\,[\text{ms}]$. We assume that membrane potentials only at odd-numbered compartments can be observable as $\boldsymbol{D}_{1:L}$. As mentioned above,

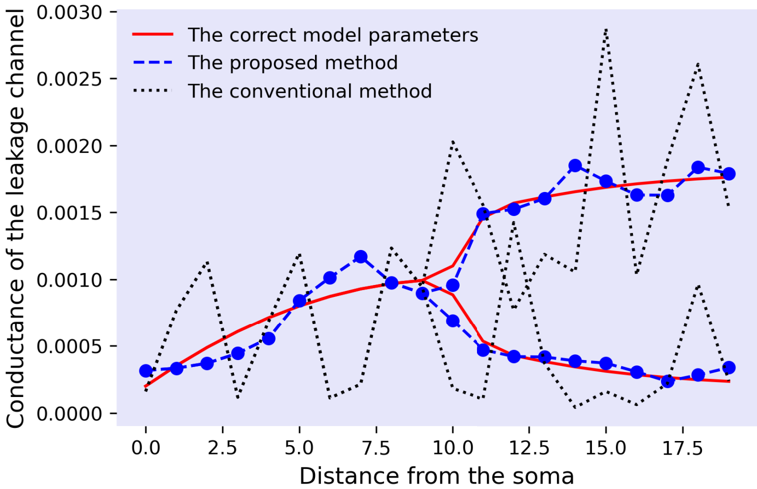

Fig. 4. Comparison of estimation results of electrical properties $\boldsymbol{\theta} = [g_L^{(1)}, ..., g_L^{(30)}]$ in the single branch neuron model. The graph shows the multi-compartment model with a branching point where distance from the soma is 10. In the graph, the correct electrical properties (red solid line), the electrical properties estimated by the MCMC (conventional method, black dotted line), the electrical properties estimated by the replica exchange method with prior considering morphological smoothness (proposed method, blue dashed line) are shown.

we estimate the conductance of the leakage channel $\boldsymbol{\theta} = [g_L^{(1)}, ..., g_L^{(30)}]$ from membrane potentials observed incompletely. In the proposed method, the iterations N is 2000 and the hyperparameters are set as $\alpha_1 = 100$, $\alpha_2 = 100$. Furthermore, we generate candidate samples by applying the following proposal distribution:

$$\rho(\boldsymbol{\theta}'_{T_i} | \boldsymbol{\theta}_{T_i}) = \mathcal{N}(\boldsymbol{\theta}_{T_i}, \Sigma) \tag{20}$$

where Σ is the variance-covariance matrix of the normal distribution. The variance-covariance matrix of the proposal distribution Σ is set as the diagonal matrix with diagonal elements all 1.0. In addition, the initial values of the replica exchange method are set as uniform distribution $\boldsymbol{\theta}[0] = [1.0 \times 10^{-3}, ..., 1.0 \times 10^{-3}]$. Finally, initial samples are discarded as the burn-in period and the estimated parameters is calculated by the expected value of remaining samples. Furthermore, the multi-compartment model parameters estimated by the proposed method are compared with the model parameters estimated by conventional method, the Markov chain Monte Carlo method (MCMC) without replica exchange [23–25]. In the conventional method, we use the same numbers of iterations as the proposed method. Furthermore, the conventional method does not have exchange of samples between different temperatures and prior information about parameters $\boldsymbol{\theta}$. Namely, in the conventional method, we assume that parameters $\boldsymbol{\theta}$ follow a uniform distribution.

Figure 4 shows the estimation results of the spatial electrical properties by using the proposed method. It can be verified the proposed method is accurate in estimating the spatial electrical properties. We compared the estimation results with the results estimated by conventional method. The results by the conventional method (Fig. 4, black dotted line) shows more fluctuating electrical properties compared with true spatial profile of electrical property. For $k \geq 10$, electrical properties are sometimes reversed compared with true ones. On the other hand, the proposed replica exchange method with prior considering morphological smoothness (Fig. 4, blue dashed line) accurately estimates the correct spatial properties. Especially for $k \geq 10$, there is the branch in the true electrical property, but the proposed method can accurately estimate the branch: properties at one branch increase, properties at the other branch decrease as the distance from the soma increases. Therefore, spatial electrical properties in the neuron model with the single branch point is estimated accurately by using membrane potentials observed incompletely.

Next, we verify generality of electrical property estimated by the proposed method. Figure 5 shows reconstruction of membrane potentials by using correct properties and estimated properties.

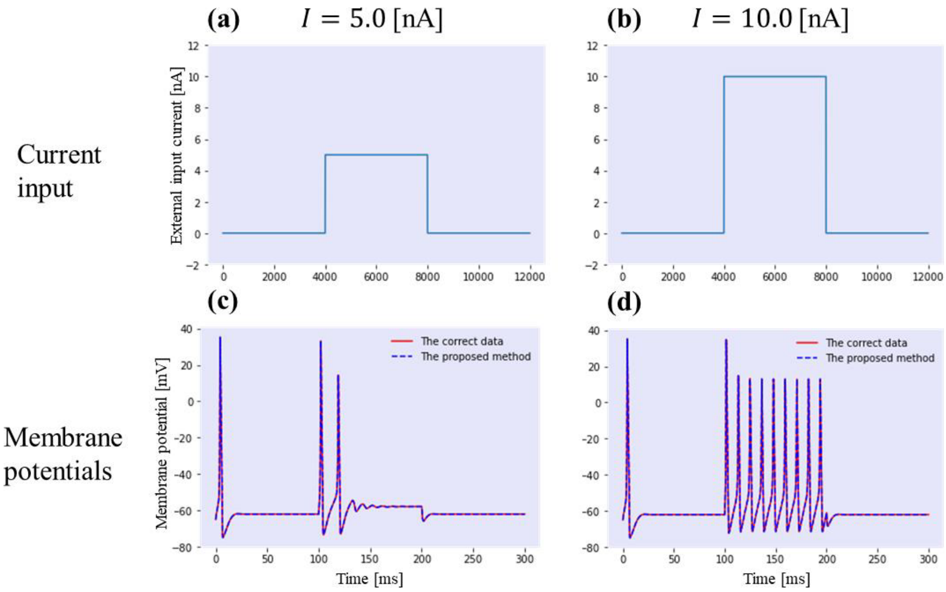

Fig. 5. Reconstructed membrane potentials simulated by using the current inputs that are not used for parameter estimation. In the graph, external input currents $I_{10}(t)$ (top) and membrane potentials calculated by using discretized differential equation in Eqs. (1)–(4) (bottom) are shown. The graph below shows reconstructed membrane potentials of correct electrical properties (red solid line) and estimated electrical properties (blue dashed line).

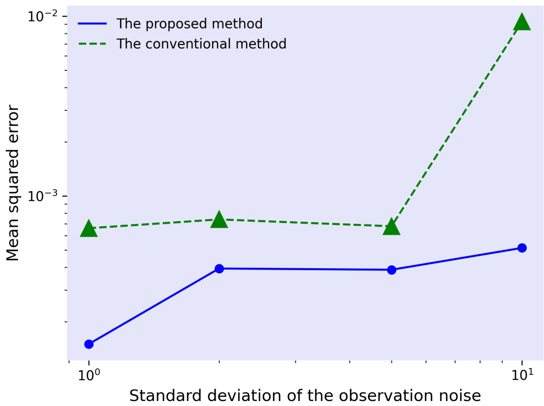

Fig. 6. Robustness to the observation noise. The mean squared error (MSE) between true and estimated electrical properties with respect to the observation noise is shown. In the graph, errors calculated by the MCMC method (the conventional method, green dashed line) and errors calculated by the replica exchange method with prior considering morphological smoothness (the proposed method, blue solid line) are shown.

We reproduce membrane potentials (Fig. 5, (c) and (d)) for correct properties and the expected value of properties estimated by the proposed method by using the current inputs $I_k = 5.0\,[\mathrm{nA}]$ (Fig. 5, (a)) and $I_k = 10.0\,[\mathrm{nA}]$ (Fig. 5, (b)) that are different from the one ($I_k = 6.0\,[\mathrm{nA}]$) used for parameter estimation. Reconstructed membrane potentials of estimated properties by using the proposed replica exchange method with prior considering morphological smoothness (Fig. 5, blue dashed line) accurately matches membrane potentials of correct properties (Fig. 5, red solid line). Especially in terms of resting membrane potential and spike timing, reconstructed membrane potentials accurately reproduce membrane potentials simulated by using correct properties. From these results, it is verified that the proposed method can accurately estimate spatial electrical properties that satisfy generality.

Furthermore, we verify robustness of the proposed method to the observation noise. Figure 6 shows mean squared error (MSE) between true and estimated electrical properties changes for different levels σ of observation noise. The results by the conventional method (Fig. 6, green dashed line) shows worse

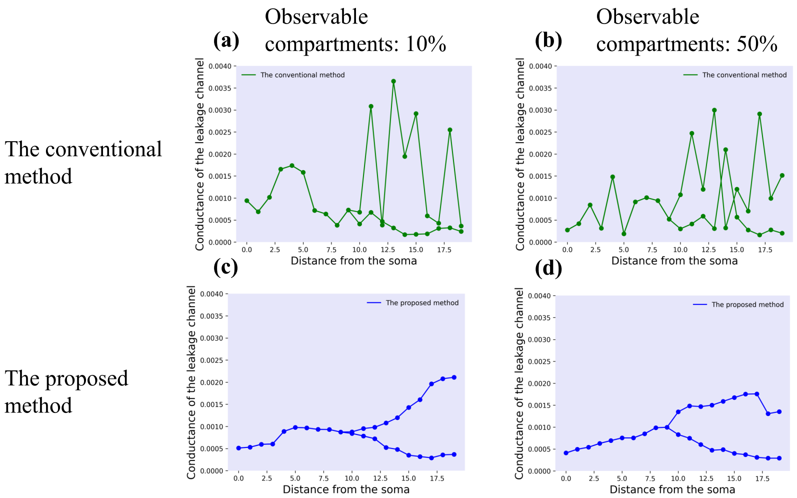

Fig. 7. Comparison of estimation results of electrical properties $\boldsymbol{\theta} = [g_L^{(1)}, ..., g_L^{(30)}]$ in the single branch neuron model. (a) and (b): Results by the conventional method. Electrical properties estimated by the conventional method in the situation where 10% of total compartments are observable ((a), MSE: 1.3×10^{-3}) and 50% of total compartments are observable ((b), MSE: 6.6×10^{-4})). (c) and (d): Results by the proposed method. Electrical properties estimated by the proposed method in the situation where 10% of total compartments are observable ((c), MSE: 2.5×10^{-4}) and 50% of total compartments are observable ((d), MSE: 1.4×10^{-4})).

estimation compared with the results by the proposed method (Fig. 6, blue solid line) in range of all noise intensity. For strong noise level ($\sigma \geq 5$), the estimation results of the conventional method are sharply worse than results for weak and moderate noise level ($\sigma < 5$). On the other hand, changes in estimation results of the proposed method due to the increase of noise level are more gradual than changes in estimation results of the conventional method. In particular, the worst estimation result of the proposed method (Fig. 6, blue solid line, σ=10) is better than the best estimation result of the conventional method (Fig. 6, green dashed line, σ=1), while the former condition of noise ($\sigma = 10$) for the proposed method is more challenging than latter condition of noise ($\sigma = 1$) for the conventional method. Therefore, the proposed method has robustness to the observation noise.

Moreover, we verify robustness of the proposed method to the number of observable compartments. Figure 7 shows comparison of estimated electrical properties in the single branch neuron model. We consider the situation where the number of observable compartments decreases. The results by the conventional method (Fig. 7(a) and (b), green solid line) shows more fluctuating electrical properties compared with true spatial profile of electrical property. On the other hand, the proposed method (Fig. 7(c) and (d), blue solid line) accurately estimates the spatial properties more accurately. In particular, the proposed method can accurately estimate the branch (Fig. 7(c), $k > 10$) even if 10% of compartments are observable. Moreover, the worst estimation result of the proposed method (Fig. 7(c)) is better than the best estimation result of the conventional method (Fig. 7(b)), while the condition of observable compartments in Fig. 7(c) is more challenging than the condition of observable compartments in Fig. 7(d). Therefore, the proposed method has robustness to the number of observable compartments.

3.2 Realistic neuron model

Finally, we estimate spatial electrical properties for conductance of leak channels $\boldsymbol{\theta} = \{g_L^{(1)}, ..., g_L^{(164)}\}$ by using the proposed method on simulation data obtained from the realistic neuron model [26]. We employ multi-compartment model with 164 compartments proposed for cortical layer 5 pyramidal neurons. As mentioned above, pyramidal cells play an important role in information transfer in the brain [3]. Therefore, it is important challenge to estimate spatial electrical property of pyramidal cells. We assume that correct spatial electrical properties of the neuron depend on the distance from soma: conductance of the leak channel sigmoidally increases. We obtain membrane potentials by simulation

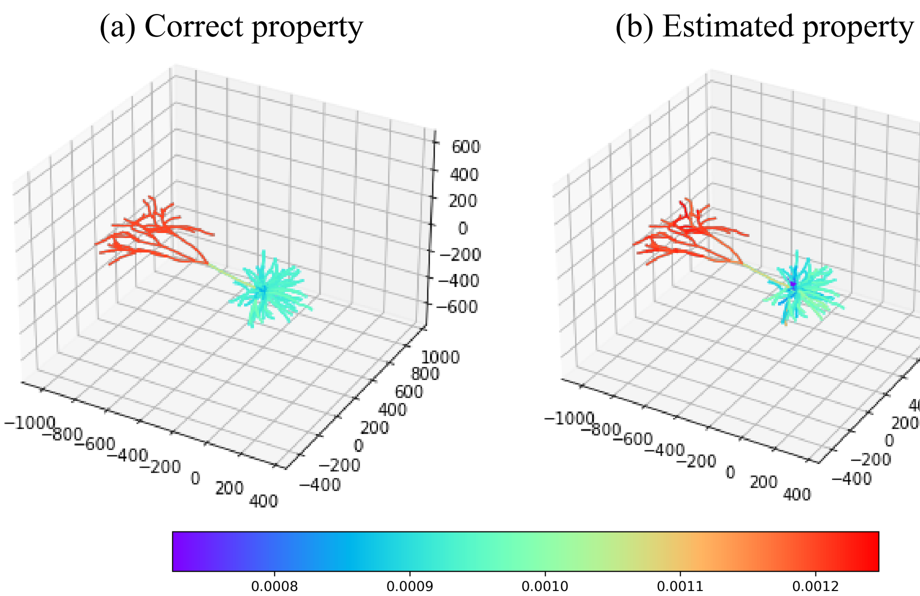

Fig. 8. Comparison of estimation results of electrical properties $\boldsymbol{\theta} = [g_L^{(1)}, ..., g_L^{(164)}]$ in the cortical layer 5 pyramidal neuron model. The graph shows the pyramidal cell described by using the multi-compartment model. In the figures (a) and (b), the correct electrical properties (a) and electrical properties estimated by the replica exchange method with prior considering morphological smoothness (proposed method, (b)) are shown. Color shows values of electrical properties.

that the four compartments are stimulated separately by $I_k(t) = 10.0\,[\mathrm{nA}]$ for 25 [ms] within 50 [ms]. We assume that membrane potentials only at odd-numbered compartments can be observable as $\boldsymbol{D}_{1:L}$. As mentioned above, we estimate the conductance of the leakage channel $\boldsymbol{\theta} = [g_L^{(1)}, ..., g_L^{(164)}]$ from membrane potentials observed incompletely. In the proposed method, the iterations N is 2000, the variance of the proposal distribution is set as $\sigma^2 = 1.0$, and the hyperparameters are set as $\alpha_1 = 1400$, $\alpha_2 = 600$. In addition, the initial values of the replica exchange method are set as uniform distribution $\boldsymbol{\theta}[0] = [1.0 \times 10^{-3}, ..., 1.0 \times 10^{-3}]$. Finally, initial samples are discarded as the burn-in period and the estimated parameters is calculated by the expected value of remaining samples.

Figure 8 shows the estimation results of the spatial electrical properties by using the proposed method. The proposed method estimate high conductance properties in the apical dendrite, low conductance properties in the basal dendrite and intermediate conductance properties in the apical trunk. We find in Fig. 8 that estimated distribution of spatial electrical properties matches true distribution. It can be verified that the proposed method is accurate in estimating the spatial electrical properties. Especially, sigmoidal change of spatial electrical properties that depends on distance from soma is accurately estimated by using the proposed method. These results show that the proposed method can estimate correct spatial electrical properties in the realistic neuron model from membrane potentials observed incompletely.

Next, we verify generality of electrical property estimated by the proposed method. Figure 9 shows reconstruction of membrane potentials by using correct properties and estimated properties. We reproduce membrane potentials (Fig. 9, bottom) for correct properties and the expected value of properties estimated by the proposed method by using the current inputs $I_k = 6.0\,[\mathrm{nA}]$ and $I_k = 12.0\,[\mathrm{nA}]$ (Fig. 9, top) that are different from the one ($I_k = 10.0\,[\mathrm{nA}]$) used for parameter estimation. Reconstructed membrane potentials of estimated properties by using the proposed replica exchange method with prior considering morphological smoothness (Fig. 9, blue dashed line) accurately matches membrane potentials of correct properties (Fig. 9, red solid line). Especially in terms of resting membrane potential and spike timing, reconstructed membrane potentials accurately reproduce membrane potentials simulated by using correct properties. From these results, it is verified that the proposed method can accurately estimate spatial electrical properties that satisfy generality for the realistic neuron model.

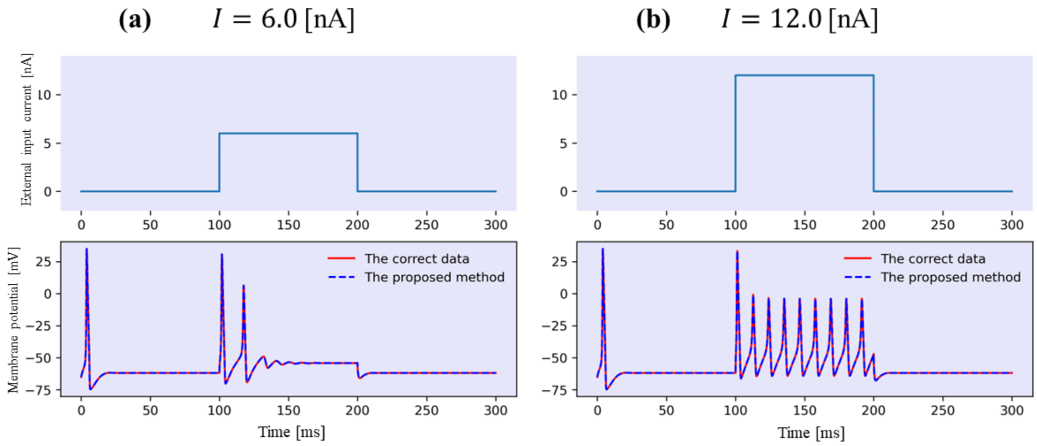

Fig. 9. Reconstructed membrane potentials simulated by using the current inputs that are not used for parameter estimation. In the graph, external input currents $I_1(t)$ (top) and membrane potentials calculated by using discretized differential equation Eqs. (1)–(4) (bottom) are shown. The graph below shows reconstructed membrane potentials of correct electrical properties (red solid line) and estimated electrical properties (blue dashed line).

4. Conclusion

In this study, we have proposed the data-driven framework for estimating the spatial electrical properties of neuron from membrane potentials observed incompletely. We have employed the multi-compartment model to consider shape of neurons and reproduce accurately nonlinear spatiotemporal electrical activity in neurons. Moreover, we have formulated the replica exchange method with the prior distribution considering morphological smoothness to solve problems: complex energy structure and incomplete observation data. The proposed method can estimate posterior distribution of spatial parameters in the multi-compartment model from observation data that is partially observable and noisy. In experiments by using simulation data obtained from the single branch neuron model and the realistic neuron model, we have verified that the proposed method can be used to estimate spatial electrical properties in the multi-compartment model. It has shown that the proposed method can more accurately estimate spatial electrical properties in multi-compartment model than the Markov chain Monte Carlo method without the prior and replica exchange. In this study, we assume that observed membrane potentials have observation noise. In addition to the observation noise, membrane potentials can have system noise due to stochastic properties of neurons that affect the stochastic behavior of dynamics of ion channels and so on. To estimate spatial electrical properties in the situation where membrane potentials have system noise and observation noise, it is essential to employ the stochastic multi-compartment model [27]; the conventional multi-compartment model follows deterministic ion channel dynamics. On the other hand, the stochastic multi-compartment model follows stochastic ion channel dynamics: each type of ion channels has multiple unitary ion channels. Each unitary ion channel follows different kinetics, and the probabilities that the states in each type of ion channels are open or close are determined by the percentage of open unitary ion channels. Membrane potentials described by the stochastic multi-compartment model can consider system noise. Therefore, by extending the proposed method to the dynamical system with the stochastic multi-compartment model, the proposed method may estimate spatial electrical properties in the situation that membrane potentials have system noise and observation noise. We leave this extension as a future work.

Acknowledgments

This work was partially supported by Grant-in-Aid for Scientific Research (B) (No. JP21H03509), and a Fund for the Promotion of Joint International Research (International Collaborative Research) (No. JP23KK0184), MEXT, Japan, CREST (No. JPMJCR1914), JST, Japan, and AMED (No. 23wm052517h0003), Japan.

References

[1] G.J. Stuart and N. Spruston, "Dendritic integration: 60 years of progress," *Nature Neuroscience*, vol. 18, pp. 1713–1721, December 2015. DOI: 10.1038/nn.4157

[2] A. Gidon, T.A. Zolnik, P. Fidzinski, F. Bolduan, A. Papoutsi, P. Poirazi, M. Holtkamp, I. Vida, and M.E. Larkum, "Dendritic action potentials and computation in human layer 2/3 cortical neurons," *Science*, vol. 367, pp. 83–87, January 2020. DOI: 10.1126/science.aax6239

[3] N. Spruston, "Pyramidal neurons: dendritic structure and synaptic integration," *Nature Reviews Neuroscience*, vol. 9, no. 3, pp. 206–221, March 2008. DOI: 10.1038/nrn2286

[4] Y. Zang, S. Dieudonné, and E.D. Schutter, "Voltage-and branch-specific climbing fiber responses in Purkinje cells," *Cell Reports*, vol. 24, no. 6, pp. 1536–1549, August 2018. DOI: 10.1016/j.celrep.2018.07.011

[5] N. Takahashi, K. Kitamura, N. Matsuo, M. Mayford, M. Kano, N. Matsuki, and Y. Ikegaya, "Locally synchronized synaptic inputs," *Science*, vol. 335, no. 20, pp. 353–356, January 2012. DOI: 10.1126/science.12103

[6] M. London and M. Häusser, "Dendritic computation," *Annual Review of Neuroscience*, vol. 28, pp. 503–532, July 2005. DOI: 10.1146/annurev.neuro.28.061604.135703

[7] H. Yamada, Y. Imaizumi, and M. Matsumoto, "Neural population dynamics underlying expected value computation," *Journal of Neuroscience*, vol. 41, no. 8, pp. 1684–1698, February 2021. DOI: 10.1523/JNEUROSCI.1987-20.2020

[8] N. Takahashi, C. Ebner, J. Sigl-Glöckner, S. Moberg, S. Nierwetberg, and M.E. Larkum, "Active dendritic currents gate descending cortical outputs in perception," *Nature Neuroscience*, vol. 23, pp. 1277–1285, October 2020. DOI: 10.1038/s41593-020-0677-8

[9] Y. Adam, J.J. Kim, S. Lou, Y. Zhao, M.E. Xie, D. Brinks, H. Wu, M.A. Mostajo-Radji, S. Kheifets, V. Parot, S. Chettih, K.J. Williams, B. Gmeiner, S.L. Farhi, L. Madisen, E.K. Buchanan, I. Kinsella, D. Zhou, L. Paninski, C.D. Harvey, H. Zeng, P. Arlotta, R.E. Campbell, and A.E. Cohen, "Voltage imaging and optogenetics reveal behaviour-dependent changes in hippocampal dynamics," *Nature*, vol. 569, pp. 413–417, May 2019. DOI: 10.1038/s41586-019-1166-7

[10] K.D. Piatkevich, S. Bensussen, H. Tseng, S.N. Shroff, V.G. Lopez-Huerta, D. Park, E.E. Jung, O.A. Shemesh, C. Straub, H.J. Gritton, M.F. Romano, E. Costa, B.L. Sabatini, Z. Fu, E.S. Boyden, and X. Han, "Population imaging of neural activity in awake behaving mice," *Nature*, vol. 574, pp. 413–417, October 2019. DOI: 10.1038/s41586-019-1641-1

[11] S. Otsuka and T. Omori, "Estimation of neuronal dynamics based on sparse modeling," *Neural Networks*, vol. 109, pp. 137–146, October 2018. DOI: 10.1016/j.neunet.2018.10.006

[12] H. Inoue, K. Hukushima, and T. Omori, "Estimation of neuronal dynamics of Izhikevich neuron models from spike-train data with particle Markov chain Monte Carlo method," *Journal of the Physical Society of Japan*, vol. 90, no. 10, 104801, September 2021. DOI: 10.7566/JPSJ.90.104801

[13] G.J. Wang, and J. Beaumont, "Parameter estimation of the Hodgkin–Huxley gating model: an inversion procedure," *SIAM Journal on Applied Mathematics*, vol. 64, no. 4, pp. 1249–1267, January 2004. DOI: 10.1137/S0036139902419826

[14] K.E. Petousakis, A.A. Apostolopoulou, and P. Poirazi, "The impact of Hodgkin-Huxley models on dendritic research," *The Journal of Physiology*, vol. 601, no. 15, pp. 3091–3102, August 2023. DOI: 10.1113/JP282756

[15] E.M. Izhikevich, "Simple model of spiking neurons," *IEEE Trans. Neural Networks*, vol. 14, no. 6, pp. 1569–1572, November 2003. DOI: 10.1109/TNN.2003.820440

[16] K. Hukushima and K. Nemoto, "Exchange Monte Carlo method and application to spin glass simulations," *Journal of the Physical Society of Japan*, vol. 65, no. 6, pp. 1604–1608, June 1996. DOI: 10.1143/JPSJ.65.1604

[17] K. Motonaka and S. Miyoshi, "Connecting PM and MAP in Bayesian spectral deconvolution by extending exchange Monte Carlo method and using multiple data sets," *Neural Networks*

journal, vol. 118, pp. 159–166, October 2019. DOI: 10.1016/j.neunet.2019.05.004

[18] G. Stuart, N. Spruston, and M. Hausser, *Dendrites*, Oxford University Press, Oxford, 2016.

[19] M.L. Hines and N.T. Carnevale, "The NEURON simulation environment," *Neural Computation*, vol. 9, no. 6, pp. 1179–1209, August 1997. DOI: 10.1162/neco.1997.9.6.1179

[20] W.J. Fitzgerald, "Markov chain Monte Carlo methods with applications to signal processing," *Signal Processing*, vol. 81, no. 1, pp. 3–18, January 2001. DOI: 10.1016/S0165-1684(00)00187-0

[21] D. Luengo, L. Martino, M. Bugallo, V. Elvira, and S. Särkkä, "A survey of Monte Carlo methods for parameter estimation," *EURASIP Journal on Advances in Signal Processing*, vol. 25, May 2020. DOI: 10.1186/s13634-020-00675-6

[22] A. Belloni and V. Chernozhukov, "On the computational complexity of MCMC-based estimators in large samples," *Annals of Statistics*, vol. 37, no. 4, pp. 2011–2055, August 2009. DOI: 10.1214/08-AOS634

[23] J. Geweke and H. Tanizaki, "Bayesian estimation of state-space models using the Metropolis-Hastings algorithm within Gibbs sampling," *Computational Statistics and Data Analysis*, vol. 37, no. 2, pp. 151–170, August 2001. DOI: 10.1016/S0167-9473(01)00009-3

[24] C.A. Kastner, A. Braumann, P.L.W. Man, S. Mosbach, G.P.E. Brownbridge, J. Akroyd, M. Kraft, and C. Himawan, "Bayesian parameter estimation for a jet-milling model using Metropolis-Hastings and Wang-Landau sampling," *Chemical Engineering Science*, vol. 89, pp. 244–257, February 2013. DOI: 10.1016/j.ces.2012.11.027

[25] R. Allison and J. Dunkley, "Comparison of sampling techniques for bayesian parameter estimation," *Monthly Notices of the Royal Astronomical Society*, vol. 437, no. 4, pp. 3918–3928, February 2014. DOI: 10.1093/mnras/stt2190

[26] Z.F. Mainen and T.J. Sejnowski, "Influence of dendritic structure on firing pattern in model neocortical neurons," *Nature*, vol. 382, pp. 363–366, July 1996. DOI: 10.1038/382363a0

[27] H.C. Tuckwell and F.Y.M. Wan, "Time to first spike in stochastic Hodgkin-Huxley systems," *Physica A: Statistical Mechanics and its Applications*, vol. 351, no. 2–4, pp. 427–438, June 2005. DOI: 10.1016/j.physa.2004.11.059